SUPPLEMENTARY DATA

Genotype-Structure-Phenotype Correlations in Disease-Associated IGF1R Variants and Similarities to Those in INSR Variants

Jun Hosoe[1], Yuki Kawashima Sonoyama[2], Fuyuki Miya[3,4,5], Hiroko Kadowaki[6], Ken Suzuki[1,7], Takashi Kato[1], Fumiko Matsuzawa[8], Sei-Ichi Aikawa[8], Yukinori Okada[7], Tatsuhiko Tsunoda[3,4,5,9], Keiichi Hanaki[10], Susumu Kanzaki[11], Nobuhiro Shojima[1], Toshimasa Yamauchi[1], Takashi Kadowaki[1,12]

[1]Department of Diabetes and Metabolic Diseases, Graduate School of Medicine, The University of Tokyo, Tokyo, Japan
[2] Division of Pediatrics and Perinatology, Faculty of Medicine Tottori University, Yonago, Japan
[3]Department of Medical Science Mathematics, Medical Research Institute, Tokyo Medical and Dental University, Tokyo, Japan
[4]Laboratory for Medical Science Mathematics, RIKEN Center for Integrative Medical Sciences, Yokohama, Japan
[5]CREST, JST, Tokyo, Japan
[6]Department of Pediatrics, Sanno Hospital, Tokyo, Japan
[7]Department of Statistical Genetics, Osaka University Graduate School of Medicine, Osaka, Japan
[8]Tokyo R&D Center, Altif Laboratories, Inc., Tokyo, Japan
[9]Laboratory for Medical Science Mathematics, Department of Biological Sciences, Graduate School of Science, The University of Tokyo, Tokyo, Japan
[10]School of Health Science, Faculty of Medicine Tottori University, Yonago, Japan
[11]Asahigawaso Rehabilitation and Medical Center, Okayama, Japan
[12]Toranomon Hospital, Tokyo, Japan

Supplementary Figure 1—Growth curve of our previously reported patient with a heterozygous missense variant (p.R739Q) of IGF1R. Height for Japanese girls (0-18 years) in 2000 is plotted on a cross-sectional growth chart.

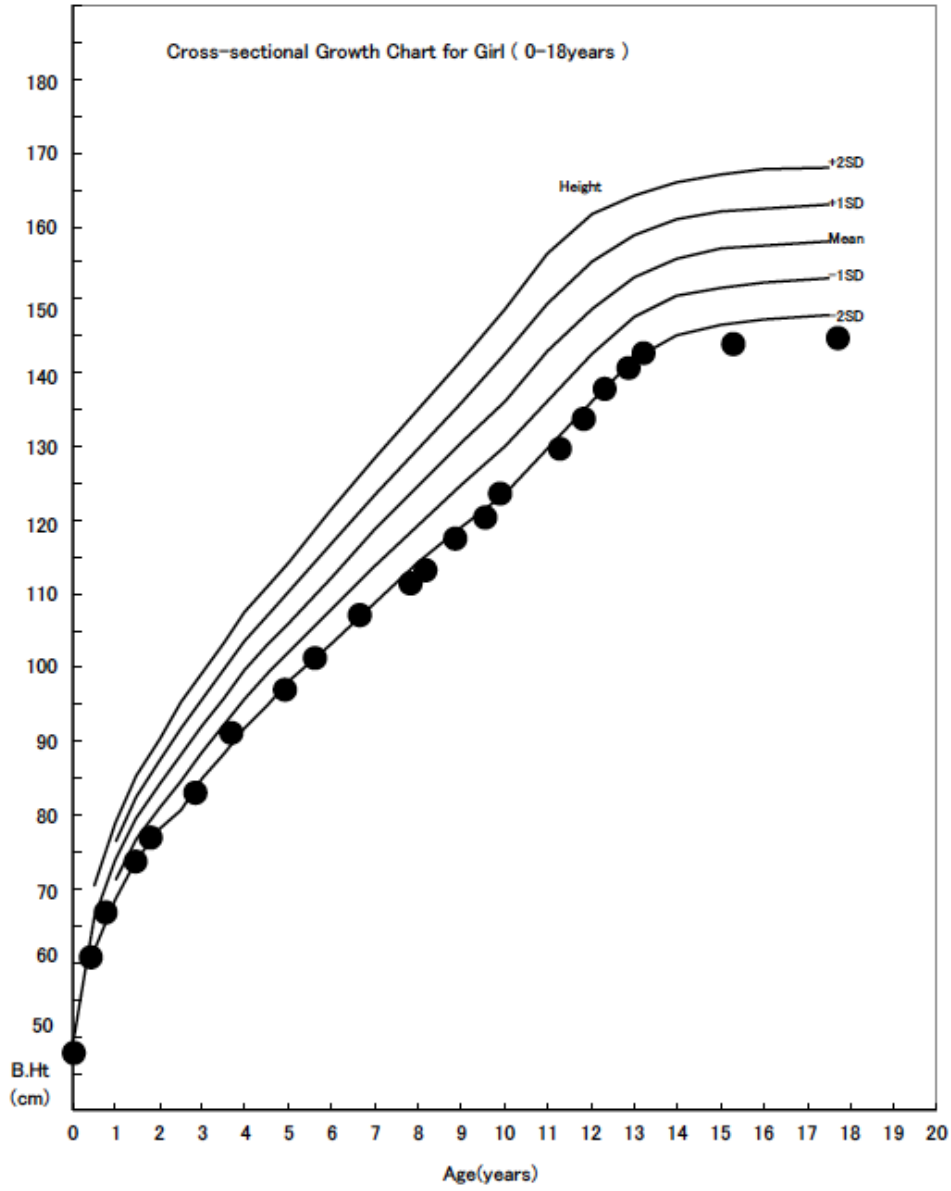

Supplementary Figure 2—Assessment of mutant IGF1R protein. ***A***: Western blotting of WT and mutant IGF1R. CHO cells were cotransfected with WT IGF1R alone, WT IGF1R/MOCK, WT/V629E, WT/K720E, WT/R739Q, WT/R739W, and WT/Y865C. Western blotting was conducted using 5 μg of total cellular protein to evaluate the levels of the proreceptor and the mature β-subunit of the receptor. ***B***: Analysis of IGF-1-stimulated autophosphorylation of the IGF1R β-subunit. Transfected CHO cells were stimulated with IGF-1 (0 and 10 nM) and the cell lysates were analyzed to detect the autophosphorylated IGF1R β-subunit by Western blotting. ***C***: Quantification of the levels of mature IGF1R β-subunit not treated with IGF-1, detected as a ratio to levels of proreceptor. The fold increase or decrease above WT was calculated. Results are shown as the mean ± SD calculated from three independent experiments. *$P < 0.05$ compared with WT. ***D***: Densitometric quantification of IGF1R autophosphorylation stimulated by 10 nM IGF-1. For mutant proteins, the percentage of the signal detected for the WT IGF1R β-subunit was calculated. Results are shown as the mean ± SD calculated from three independent experiments. *$P < 0.05$ compared with WT.

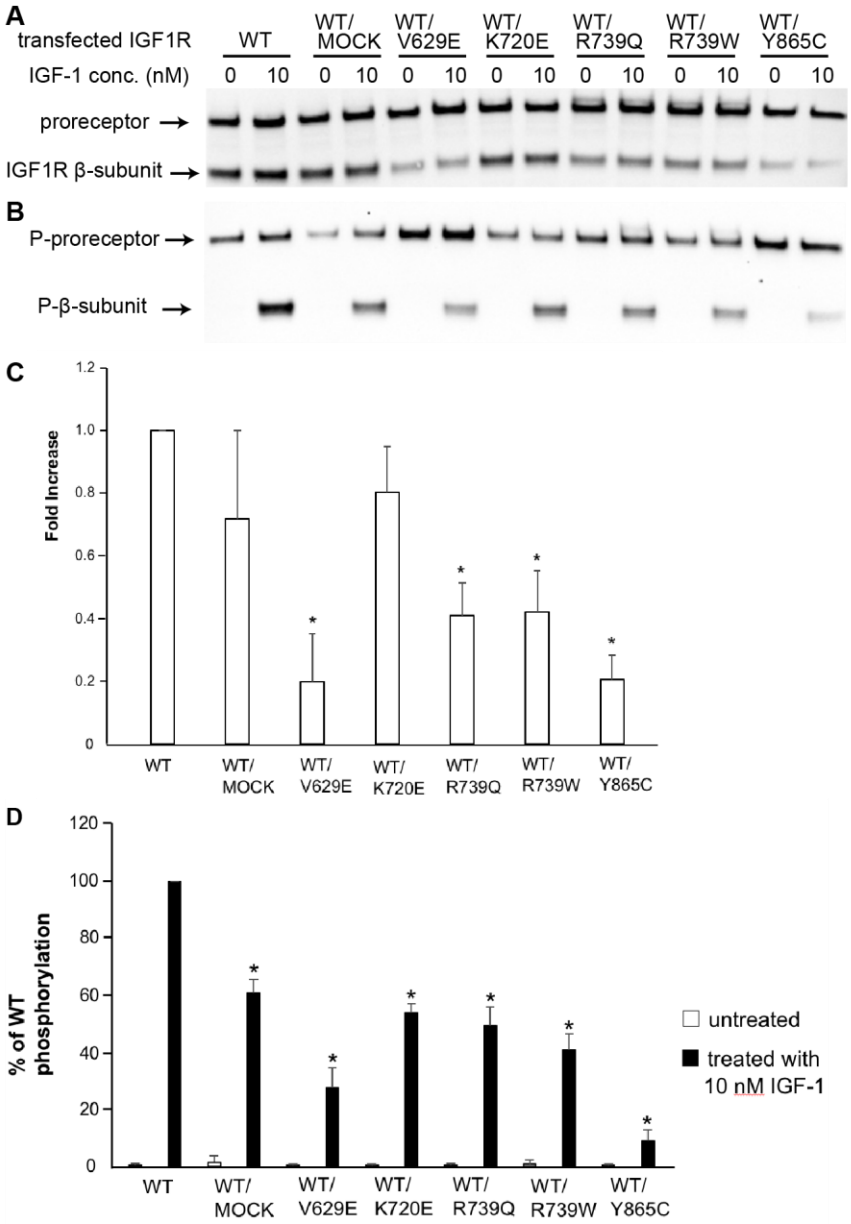

Supplementary Figure 3—Simplified representation of the putative folding nucleus of IGF1R FnIII-2 (A) and FnIII-3 (B) structures. (Upper panel) FnIII-2 and FnIII-3 of IGF1R are formed by seven β-strands accounting for two β-sheets. Green triangles show the four residues constituting the folding nucleus of FnIII-2 and FnIII-3. Magenta pins indicate the loci of missense variants leading to growth retardation and blue pin indicates the likely benign variant. (Lower panel) Simplified view of IGF1R FnIII-2 and FnIII-3 (left) and TNfn3 (right), the most extensively studied of the typical FnIII domains. The core of each protein consists of six layers, while the four residues form the folding nucleus (green circle). The core of each domain is shown to consist of six layers with the four key residues forming the folding nucleus presented in green circle. The hydrophobic core of FnIII (corresponding to the yellow residues in layers 2-4 of strands B, C, E, and F) is the key residues for stabilizing the FnIII structure.

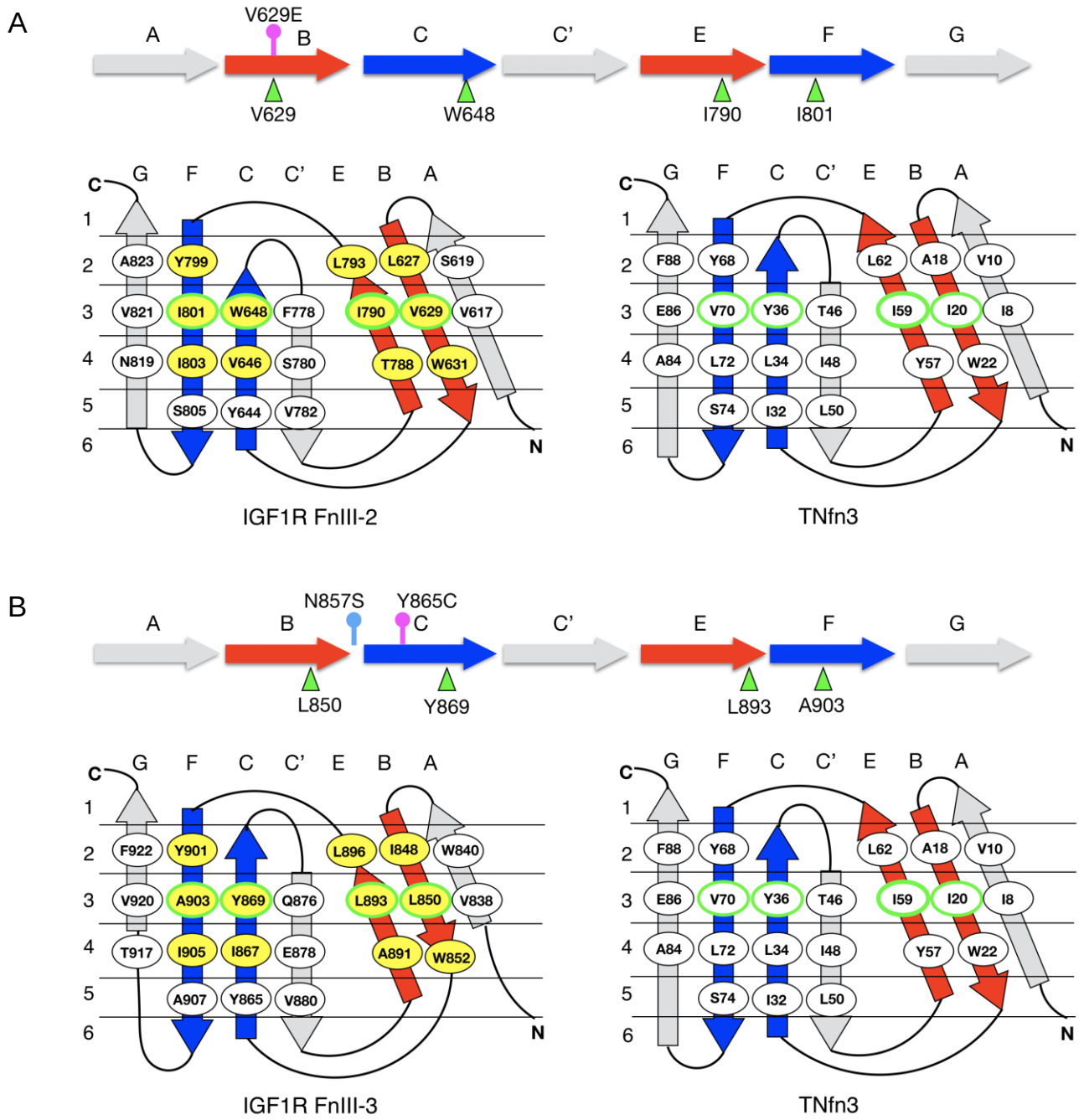

Supplementary Figure 4—Orthogonal views of the folding nucleus of FnIII-2 and FnIII-3 of IGF1R compared to that of TNfn3. The folding nucleus of FnIII-2 in IGF1R is formed by residues V629, W648, I790, and I801 corresponding to I20, Y36, I59, and V70 in the core of TNfn3, while the folding nucleus of fnIII-3 in IGF1R is formed by residues L850, Y869, L893, and A903 corresponding to I20, Y36, I59, and V70 in the core of TNfn3. These four residues are positioned in the strands B, C, E, and F in the same core layer. The β-strands B and E are shown in red, while the β-strands C and F constituting the common hydrophobic core of the FnIII domains are shown in blue.

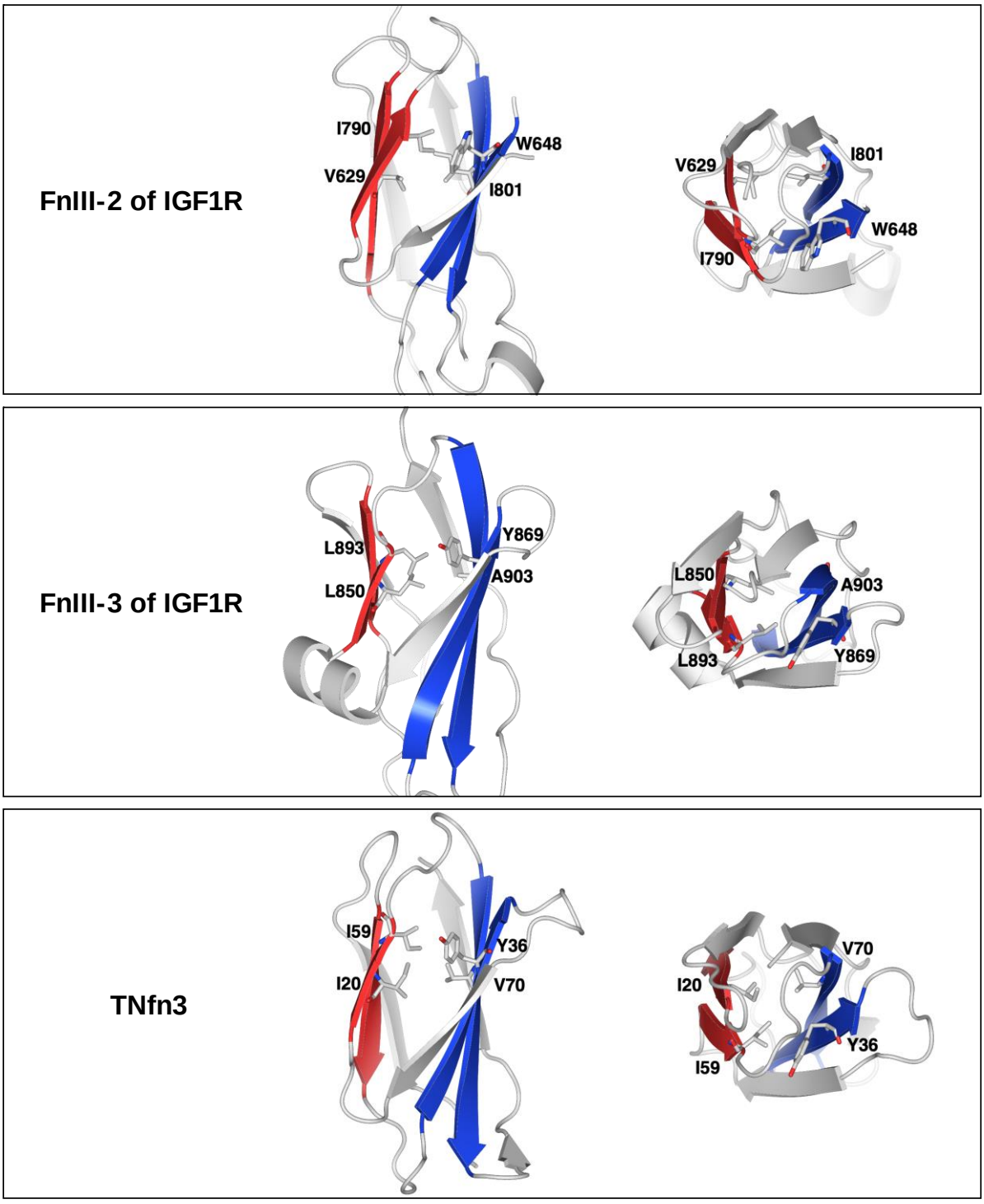

Supplementary Figure 5—Structures of FnIII-2 (except for the insert domain) and FnIII-3 of IGF1R and locations of missense variants of FnIII. The residues affected by the mutants leading to growth retardation and the likely benign variant are green and light blue, respectively. The β-strands B and E are shown in red, and the β-strands C and F constituting the common hydrophobic core of the FnIII domains are shown in blue.

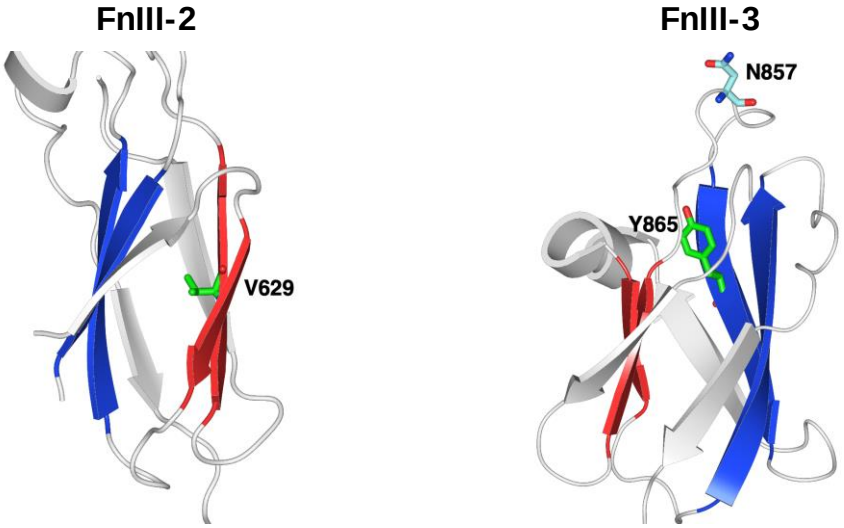

Supplementary Figure 6—Structural changes introduced by the variant (K720E) located in αCT of IGF1R of the active conformation. In the active conformation of IGF1R dimer and IGF-2 complex (PDB ID: 6VWI), the IGF-2 binding site is formed by the L1 domain of one protomer and the αCT and FnIII-1 domains of the other. The side-chain of K720 in the αCT forms a salt-bridge with D519 in the FnIII-1 (blue dash line), stabilizing a spatial αCT position and forming the IGF-2 binding site. Substitution K720 by glutamic acid with a negatively charged side-chain leads to disruption of the salt bridge and electrostatic repulsion with D519. ***A*:** Structure of the binding region of IGF-2 in IGF1R. IGF1R and IGF-2 (blue) in ribbon representation. K720 (green), E720 (magenta) in αCT and D519 (gray) in FnIII-1 are presented as sticks. ***B*:** K720 (green), E720 (magenta) in αCT and D519 (gray) in FnIII-1 are shown as sticks and space-filling models. ***C*:** Cartoon representation of an arrangement of the αCT, FnIII-1 domain and IGF-2 in IGF1R dimer and IGF-2 complex. K720 is deduced to contribute to keeping the spatial αCT position to stabilize the IGF-2 binding site in the active form.